Forces in the Brownian World

Luc Pierre Faucheux

January 1995

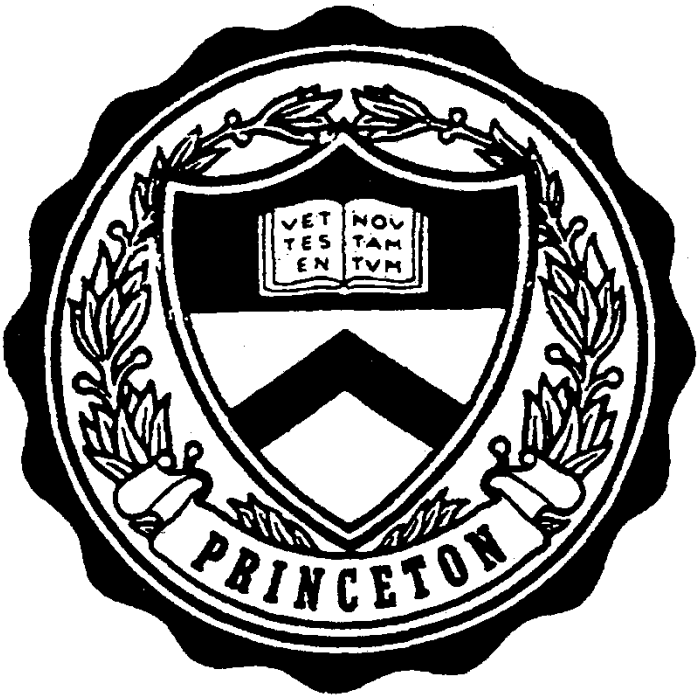

Ph.D. Thesis
Physics Department
Princeton University

Forces in the Brownian World

Luc Pierre Faucheux

A DISSERTATION
PRESENTED TO THE FACULTY
OF PRINCETON UNIVERSITY
IN CANDIDACY FOR THE DEGREE
OF DOCTOR OF PHILOSOPHY

RECOMMENDED FOR ACCEPTANCE
BY THE DEPARTMENT OF PHYSICS

January 1995

Table of Contents

Chapter V
External forcing and particles Separation

We showed in the previous chapter that building a thermal ratchet with optical tweezers is rather unpractical for particle separation. In particular, one can trap only one particle at a time, and has to resort to a sophisticated optical setup. Following here a suggestion from Jacques Prost, we tried to build a device that requires only a single function generator. The one dimensional periodic asymmetric potential is produced by a applying an electric field through electrodes deposited on a glass substrate in the right fashion. In such a system, many particles can be trapped at the same time.

We first tried to build such an engine on the premises of a DC electric field. I describe in section A the principle of this electrophoretic pump, the setup and the problems encountered. Because of the strong counter electric field produced by the ions in water, we could not get this system to work.

We resorted to work with AC fields (frequency 100 kHz). I describe in section B the principle of this dielectrophoretic pump, and the particular setup. We show the existence of an induced drift and discuss the possibility of particle separation.

A Electrophoresis

A 1 Principle of a thermal ratchet

The principle underlying a thermal ratchet has been described in Chapter IV. It comes down to producing a periodic asymmetric potential as shown in Figure **V-1**.

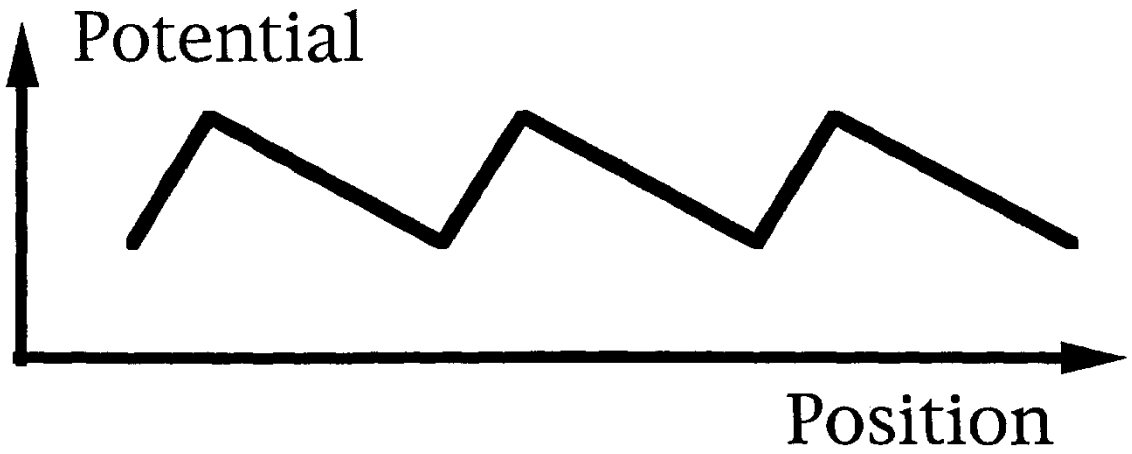

Figure **V-1:** The keystone of a thermal ratchet: a one dimensional periodic asymmetric potential.

Because polystyrene or silica spheres in water are naturally charged, we first tried to produce this potential with a DC electric field. In that case the potential profile shown in Figure **V-1** is produced by an electrostatic potential having the same characteristic: one dimensional periodic asymmetric. Let me now describe the setup.

A 2 Setup

A2a lithography technique

Lithography is a well known technique used to deposit metallic films on substrates in a precise way, build electronic components on a chip layer by layer, and even build micro-motors.

Let us suppose that one wants to evaporate a metal, say gold, on a glass substrate, so as to make a vertical line. I show in Figure **V - 2** the steps involved in this process. In **a**) a glass plate is thoroughly cleaned. In **b**) a layer of photoresist is deposited onto the glass plate. In **c**) a dark mask is applied onto the photoresist layer. In our case this mask is a thin vertical band placed in the middle of the plate. This mask is usually made out of a thin paper, photo negative or metal sheet. It has to be opaque to ultraviolet light. The sample is then subjected to radiation in the ultraviolet frequency range. The photoresist exposed to this radiation will become more resistant, and will stick to the glass plate. The mask is then taken out and the sample is washed in a mild acid bath: this takes out the part of the photoresist not exposed to the UV light (in our case a thin vertical band as shown in **d**). In **e**), the sample is then placed is a vacuum chamber and a gold film is deposited onto it, usually by evaporation technique. As a result, the whole sample is covered with a thin metallic film shown in gray in **e**). In **f**), the sample is washed with a more concentrated solution of acid than in **d**). This takes out all of the photoresist. The metallic film deposited onto the photoresist goes out with it, the one deposited onto the glass plate stays. The end result shown in **f**), is a glass plate with a thin vertical band of gold in its middle.

The resolution one can get with this technique is of the order of one micron. (it is roughly set by the wavelength of the radiation used, the thickness of the deposited metal film, and the mechanical properties of the photoresist used). The lithography technique requires, however, a lot of experience. We thus decided to ask a c o m p any[1] to do the job for us after we provided them with the design and specifications of the desired patterns. The chairman of the company, Saleem Shaikh, proved himself to be extremely competent and willing to accommodate our ever-changing requests. This part of the thesis would certainly not exist without him.

[1] Thin Film Devices, Inc., 1180 N Tustin Av., Anaheim, CA 92807.

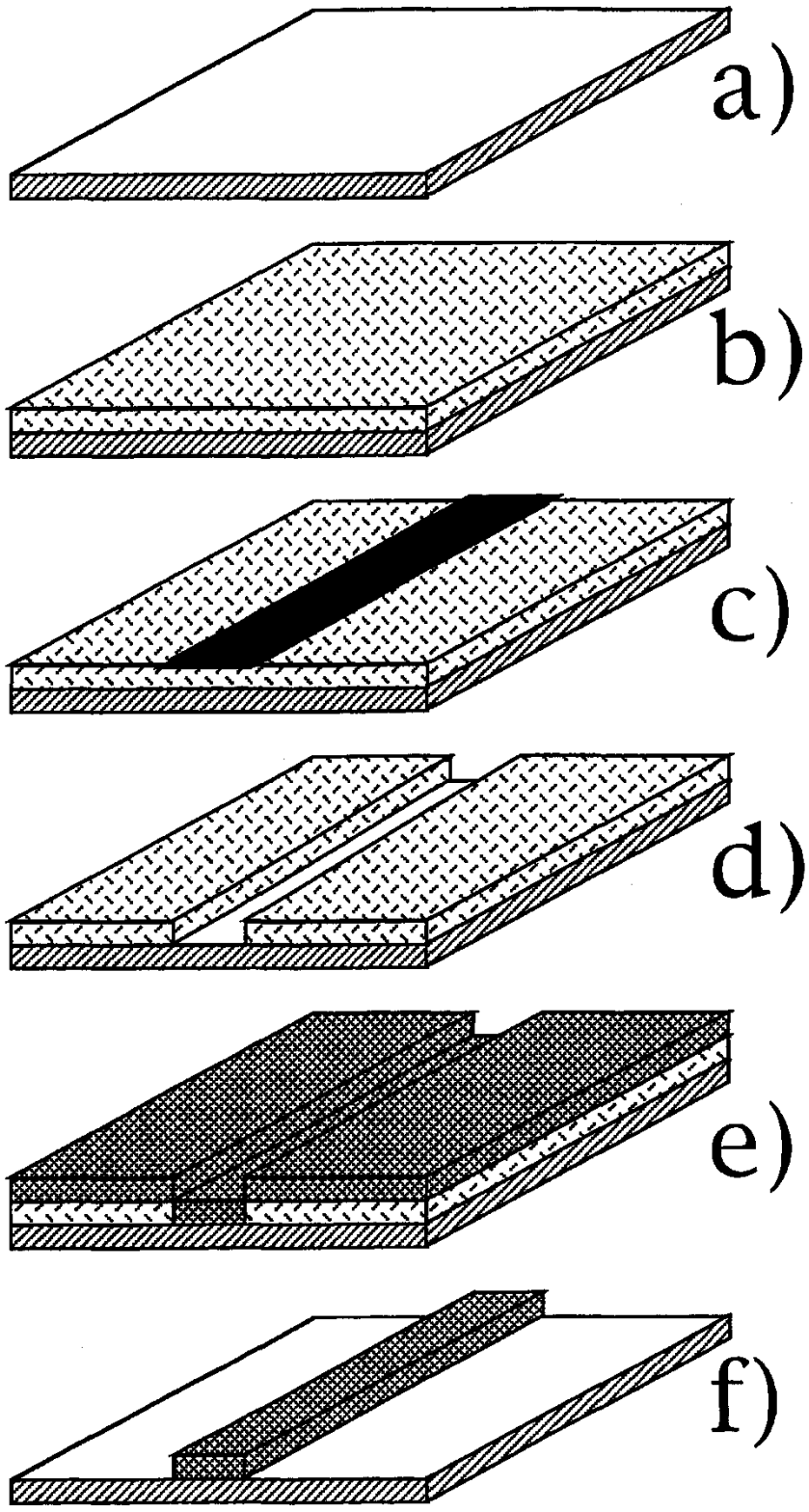

Figure **V-2**: The steps involved in depositing a metallic film on a glass substrate so as to create a vertical line.

A 2 b February 1993: the ITO[2] experiment

This first stage of the experiment was done by Adam Simon in collaboration with Albrecht Ott and Akiva Dickstein at NECI Research Institute, the author of this thesis being at that time still looking at Brownian trajectories on a computer screen in the basement of the Princeton University Physics Department, not too far away.

The design of the cell is shown in Figure **V - 3**, as well as a blow-up of the central region. The idea is to create a periodic asymmetric succession of thin electrodes along one axis of the glass plate. The periodicity of the pattern is 19 microns, the distance between fingers is 5 and 10 microns respectively. The asymmetry factor is then 2. The width of the fingers is 2 microns, and their thickness is 0.3 microns. The length of the fingers is 0.96 mm. The large ratio of their length to the spatial period makes the potential profile effectively one dimensional when applying a DC field between the interdigited fingers. The metallic film deposited onto the glass plate is made out of Indium Tin Oxide (ITO). This particular material was chosen because it is transparent in the visible, and allows observation of the Brownian particles even if they lie on top of the metallic film.

A2c sample preparation

The electrodes were connected to a function generator[3] by two thin wires, glued to the glass plate by five minutes epoxy[4]. The electric contact was achieved by a silver liquid paint[5]. The particles used are of diameter ranging from 1 to 3 microns, made out of silica

---

[2] nothing to do with the Ito-Stratonovitch controversy (Appendix B)!

[3] Synthesizer model 3325B from Hewlett Packard Corp., Sunnyvale, CA.

[4] Fast Epoxy from Devcon Corp., Danvers, MA.

[5] Colloidal silver liquid #12630 from Electron Microscopy Sciences, Ft Washington, PA.

or polystyrene[6]. They are usually diluted in pure water down to volume fraction of around 10^{-2}.

The cells are closed on top by a coverslip number 0, and sealed by fast epoxy, wax, Torr seal[7], or nail polish[8]. The spacers used were mylar sheets, parafilm, or thin metallic wires of calibrated diameters[9].

The sample is observed under the bright field illumination on an inverted microscope[10] with long working distance objectives of moderate magnification (X40 at most[11]). One wants at the same time to resolve the 1.5 microns diameter particles and keep a field of view large enough to observe many particles and grid periods. The total field of view was chosen to be around 120 microns by 150 microns.

At first, the particle suspensions showed no response whatsoever to the applied electric field. Much time was lost in trying to find a correct surface treatment of the particles that will lead to a noticeable effect. Painstaking surface treatment of the particles with polymers[12], of the glass plate with a silica film showed no improvements. Replacing water by octane, a less polar fluid where the Debye screening length for DC field is larger, did not give any results.

[6] Bangs Laboratories, Inc., Carmel, IN.
[7] low vapor pressure resin from Varian Associates, Lexington, MA.
[8] Nail enamel hypo-allergenic "Soft Spice" from Almay Inc., NY.
[9] Tungsten wires from California Fine Wires Company, Grover City, CA.
[10] IMT-2 from Olympus, Inc., Lake Success, NY.
[11] ULWD CD Plan 40 PL from Olympus, Lake Success, NY.
[12] ZLI-3124 from EM Industries, Inc., Hawthorne, NY.

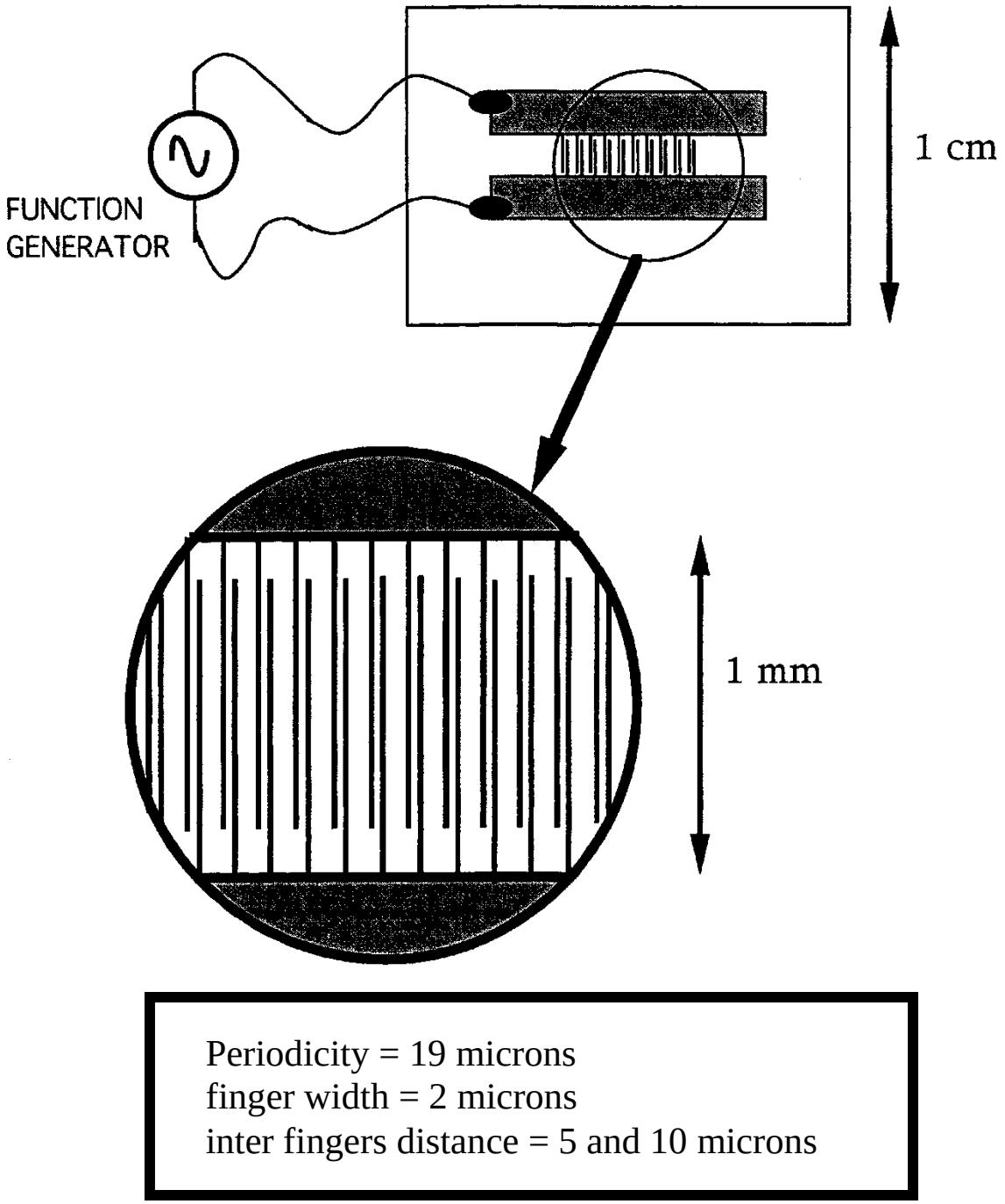

Figure **V - 3**: Geometry of the electrophoretic pump. The metallic film is either Indium Tin Oxide of thickness 300 Å, or gold of thickness 1500 Å.

We suddenly realized that the high resistivity of ITO (bulk resistivity=10^{-3} ohm.cm) combined with the small thickness of the film was such that the applied voltage at the level of the electrodes was essentially down to zero. The resistance of the interdigited fingers was of order a few hundreds of MegOhms.

A 2 d August 1993: Going for the gold!

We then decided to invest in a new set of "grids", as we got used to call them, this time made out of gold (bulk resistivity= 10^{-5} ohm.cm), of large enough thickness so that the potential from the function generator will be transmitted almost entirely to the electrodes in solution. The design of this new batch is shown in Figure **V-3**, we just decided to change the evaporated material. The resistance of the electrodes was this time of order a few Ohms. The first try was almost a success! The particles responded to the electric field in the desired way: they were attracted to the grounded electrodes when applying a voltage.

A few improvements were still needed. The particle would tend to get irreversibly stuck to the electrodes for applied voltages above 100 mV. We decided to treat the surface of the sample with a silica film[13], thus creating a dielectric isolating layer between the metallic electrodes and the particles in solution. The thickness of this silica film had to be carefully chosen: making it too thick will completely screen the field created by the electrodes. Making it too thin will not prevent the particle to stick to the electrodes. Some time was spent into figuring out the right thickness. It is of order one micron, and the film is deposited onto the glass plate by spinning the plate at 3 krpm on a spin coater[14], and dropping with a Pasteur pipette 12 drops of Silica Film every ten seconds. Ten seconds between drops was long enough to let the solvent evaporate and leave only the silica layer on the plate.

---

[13] SilicaFilm from Emulsitone Co., Whippany, NJ.

[14] Photo Resist Spinner EC1O1DT from Headway Research, Garland, TX.

A 3 Counterions

However, if we were able to attract the particles in the minimum of the electrostatic potential (see Figure V-i), switching off the potential will bring them back to their initial position! The principle of the thermal ratchet (where the particles have to be free to diffuse once the potential is switched off) was defeated.

This is due to the presence in solution of counterions. The solution is globally electrically neutral. If we are able to attract the charged particles to the potential minimums (Figure V-i), it also means that we attract to the potential peaks ions of opposite charges. This creates in solution a charge distribution. The electrical field from this charge distribution opposes the applied field and is thus called counter field. Switching off the applied field allows this charge distribution to relax back to its initial state, and brings back the particles to their initial positions!

We tried to answer this problem by adding to the water an electrophoretic gel (Agarose[15]) used in chromatography to stabilize the electrophoretic response of the ions in solution. Ions exchange resin was also tried to try to get as pure a solution as possible, with no visible effect. A more promising perspective seemed at that time to produce an asymmetry in time in the on and off switching of the applied potential. Instead of swiftly switching it off once the particles are attracted to the potential minimum, we tried to slowly decrease it back to zero. The idea was to let the counterions, much smaller than the particles, diffuse homogeneously in solution while still holding the particles in the minimum of potentials. We realized after some time that this would not work either: the problem is symmetric in the particles and counterions: if the particles are trapped, the

15 Agarose of type IV-A, 11-A and I-A dissolved in a 10^{-2} M water solution, from Sigma Chemical Company, St Louis, MO.

counterions are also trapped by the same amount, however slowly the trapping force is modulated.

By that time, the optical tweezer technique described in Chapter IV started to show much cleaner effects than the often confusing electrophoretic effects observed, and we decided to switch to a completely different setup, relying on dielectrophoretic effects (induced dipole of the particles as opposed to their permanent charges).

B Dielectrophoresis

B 1 Principle

The principle of dielectrophoresis is similar to the optical tweezing techniques described in chapter IV, except that the frequency of the applied electric field is now of order 100 kHz instead of $10^{1\ 4}$ Hz (infrared spectrum). Dielectric particles are trapped in the regions of highest intensity, if their refractive index for the frequency considered is larger than water.

B2 Setup

We could not use the previously used grids: they are such that the electrostatic potential is periodic and asymmetric. The electric field (spatial derivative of the potential) is thus also periodic, but looses the asymmetry. The intensity is the square of the electric field and is also periodic symmetric. We have to resort to a different setup, so as to produce a periodic asymmetric profile for the intensity. Following the lines of Rousselet et al. (1994) we chose the configuration shown in Figure **V-4**. The general design is the same as that in Figure **V-3**, with the exception that the asymmetry is now in the vertical direction. Each finger shows a "Christmas tree" structure. Note that the distance between fingers is now a constant (50 microns).

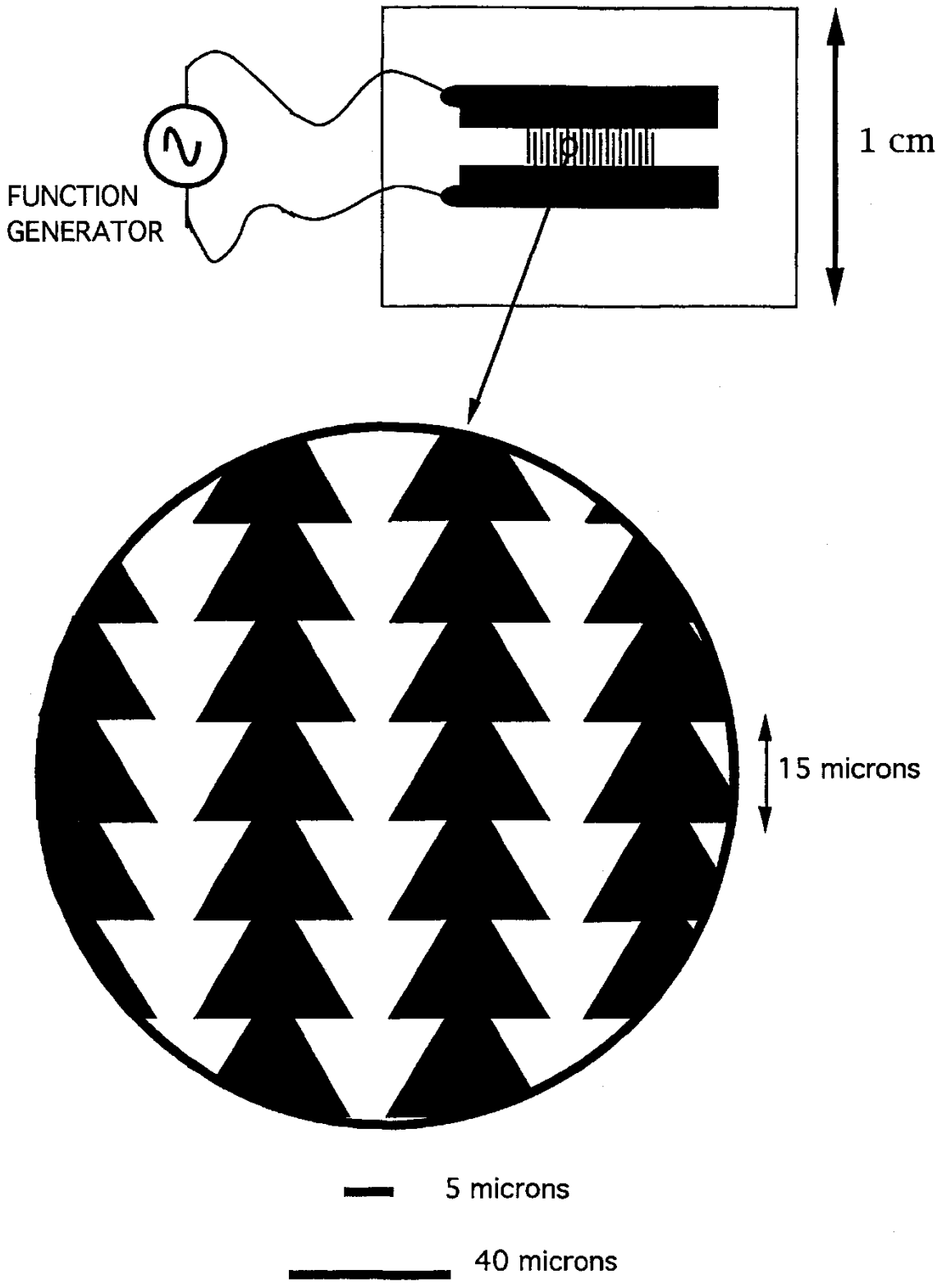

Figure **V-4**: Geometry of the dielectrophoretic pump. The thickness of the deposited gold film is 1500 Å.

When applying a fixed potential, the electric field is roughly inversely proportional to the distance between the two electrodes (just as in a capacitor). Curvature effects at the tip also increases the value of the electric field. The region of highest intensity will then be between the two tips of the triangles. Because of the asymmetry of the design in the vertical direction in Figure **V-4**, the profile of intensity along the vertical direction between two fingers will present the required characteristics of a thermal ratchet: periodic and asymmetric.

Working in the frequency range of order 100 kHz avoids the electrophoretic problems such as ions injections and electrodes current. Some time was spent to figure out the best way to seal the cell. Five minutes epoxy tends to leach too many ions in solution, which degrades the response of the sample after a few minutes. Having more ions in solution forces us to go to higher voltage in order to get the same response from the particles. We quickly reach voltages (of order 3 V in our system) where electrolysis of the water would occur. After many tries (Torr seal, wax, grease) we found that nail polish was actually the best solution[16]. Also, nail polish does not dry completely even after a few hours, which allows us to clean the gold electrodes and reuse them.

The first few tries were done in pure water. As expected, the particle gets trapped between the tip when the AC voltage (of order 200 mV) is applied. This is shown in Figure **V-5**. When switching off the field, they would diffuse freely from their trapped position. The problem of the counter field was solved!

[16] L. Salome, private communication.

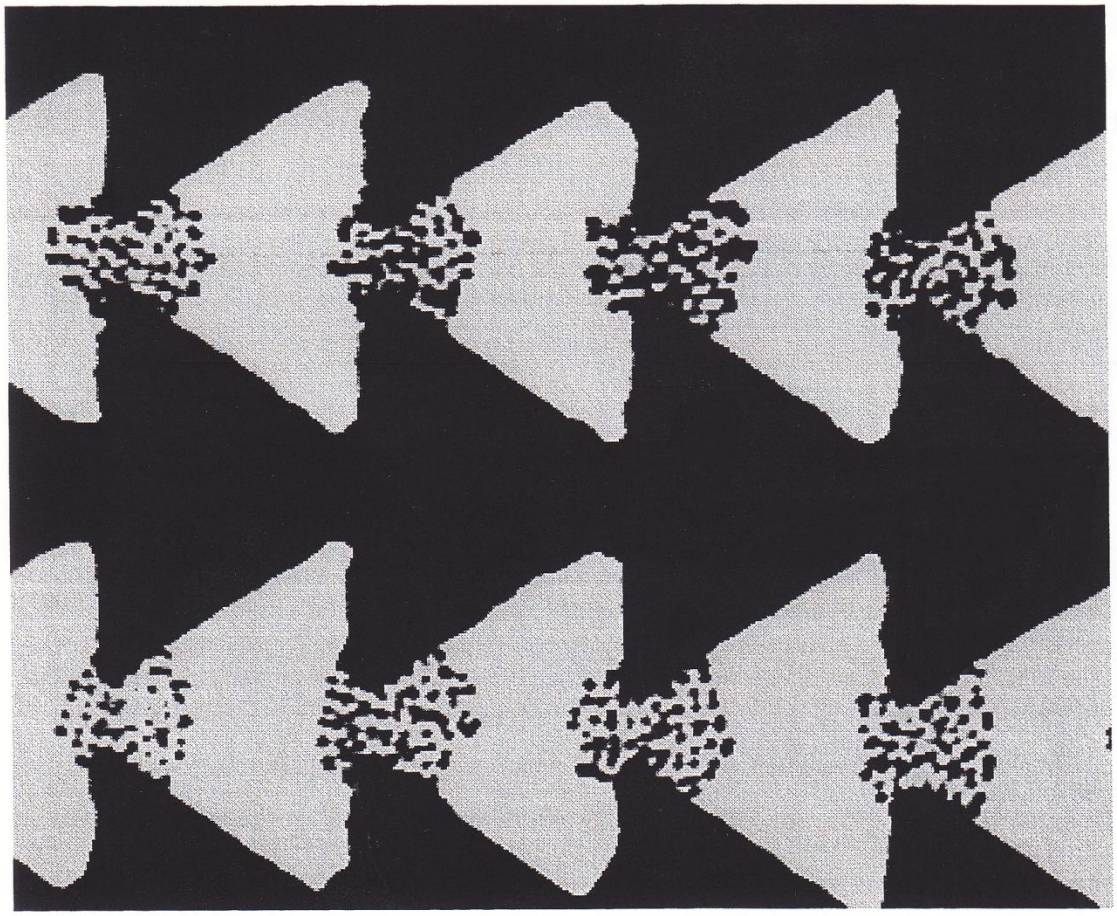

Figure **V-5**: The 1.5 microns diameter silica particle are trapped between the triangle tips (regions of highest intensity) when applying a DC field (frequency=100 kHz, magnitude=l V). This situation corresponds to pure water. Full horizontal scale=60 microns. The black regions correspond to the gold electrodes. Particle induced motion is from right to left.

However, after a few minutes, the particles would not be trapped anymore between the tips, but would form a banana shape object between the two dips of the triangles. This is shown in Figure **V-6**. This was due to ions injection into the water from the nail polish or fast epoxy. Injections of ions increases the water refractive index for the frequency we are dealing with (100 kHz), in accordance with the Clausius-Mossotti relation (Feynman 1964, section 32-5). This refractive index actually becomes larger than the refractive index of the silica particles, which are no longer trapped in the regions of highest intensity, but in the ones of lowest intensity.

They then gather on the boundary between the two high intensity regions of each well. Note that the asymmetry of the intensity profile is clearly apparent in Figure **V-6** from the curved form (banana shape) of the band of particles.

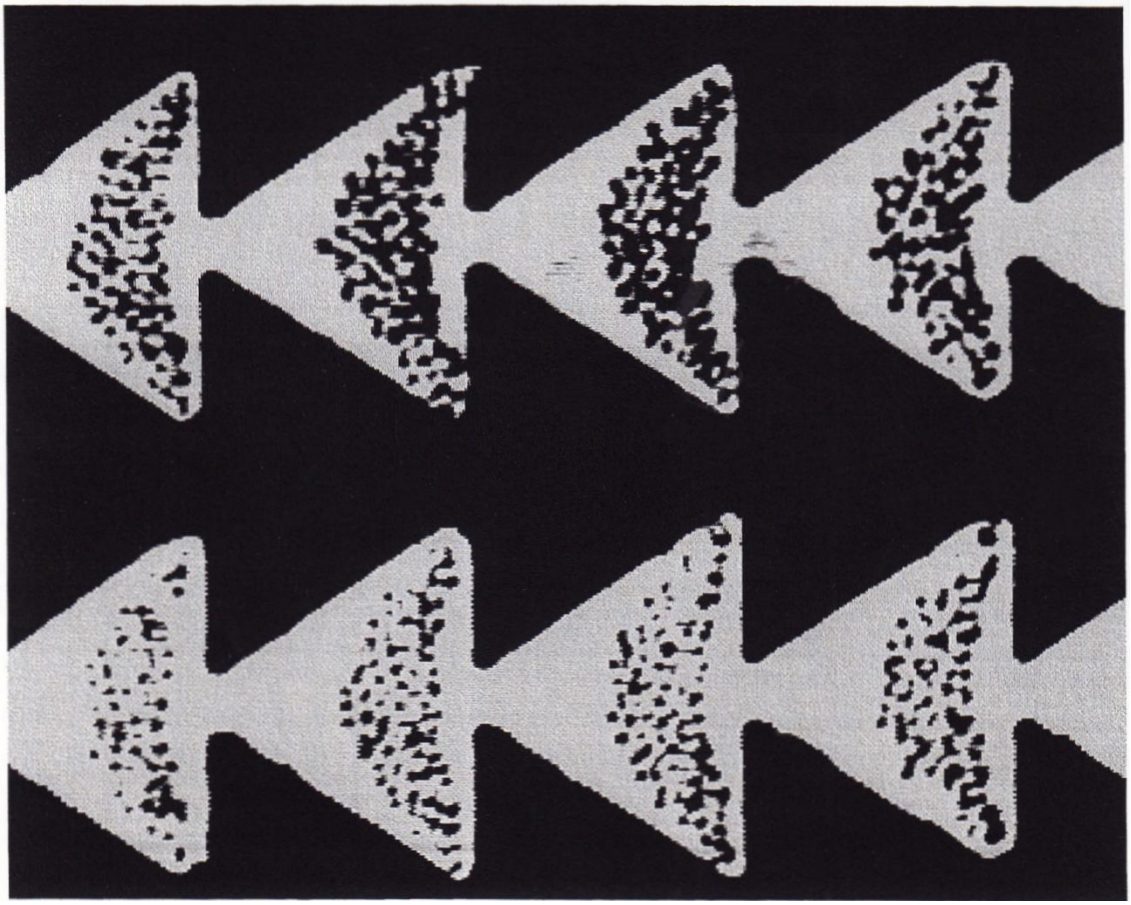

Figure **V-6**: The 1.5 microns diameter silica particles are trapped between the triangle dips (regions of minimum intensity) when applying the DC field (frequency=100 kHz, magnitude=1 V). This situation correspond to an ionic solution. Full horizontal scale=70 microns. The black regions correspond to the gold electrodes. Particle induced motion is from left to right.

How does this effect change our problem? First, the position of the trap is different. However, the profile of trapping potential has the same characteristics than the profile of intensity (since it is exactly its symmetric): periodic and asymmetric. This is enough for a thermal ratchet to work. From switching off the applied AC potential during a time τ_{off} and switching it back on, we are able to

observe a net drift of particles in the expected direction. The drift probability is defined as the average number of particles advancing by one period at each modulation, divided by the total number of particles in the trap. It is plotted in Figure **V-7** as a function of the off time τ_{off}. An experiment would run for two hours maximum. We checked that during this time the behavior and the response of the particles did not change enough to affect significantly our measurements.

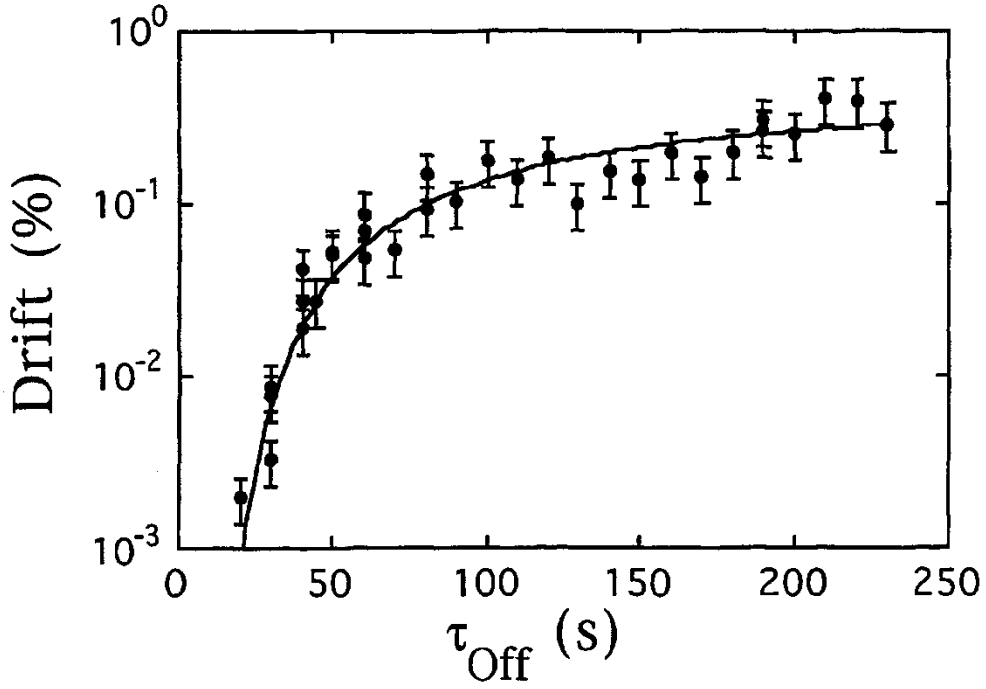

Figure **V-7**: The fraction of particles (1.5 microns diameter silica spheres) drifting forwards as a function of the off time in seconds. The solid line comes from fitting equation (Vi) to the experimental points.

B 3 Discussion

Let us now discuss this curve in more detail. The value of the drift starts from zero at the origin, and saturates to a value close to 1/2. For short off times τ_{off} the particles do not have enough time to diffuse to the next well. Measurements for time scales above three minutes become uncertain because we cannot track the particles when they diffuse above the gold electrodes (in the region where we do not observe them anymore). In this experiment, we do not measure any significant number of particles drifting backwards. The drift is thus equal to the probability for particles to diffuse forwards to the next well, called forwards probability P_f. From Chapter IV equations (IV2a), the experimental points are fitted by the function:

$$P_f = \frac{1}{2}.\exp\left[\frac{-\tau_f}{\tau_{off}}\right] \qquad \text{(V1)}$$

This defines a characteristic time scale $\tau_f \approx 130$s. From the value of the diffusion coefficient D of a 1.5 microns diameter particle, the corresponding diffusion length $\lambda_f = \sqrt{2D\tau_f}$ is of order 5 microns. Hydrodynamic interactions between particles is neglected in the above estimate. We however included the hydrodynamic correction due to the bottom plate of the cell (see Chapter III). This amounts to divide the diffusion coefficient by a factor 3. We also assumed that the saturation value of the forwards probability was (1/2) as in Chapter IV. We now discuss these assumptions.

As opposed to Chapter IV figure **IV-16**, one does not observe any decrease of the drift for long time scales. This could be due to a limitation of our measurements. Since the forwards diffusion length is of order 5 microns, and the spatial period 15 microns, the backwards diffusion length is of order 10 microns. The corresponding backwards characteristic time is then of order 520 s, out of our experimental range. However, the potential asymmetry $\alpha = (\tau_b / \tau_f)$ is in our case around 4. From Figure **IV-17**, the maximum value of the drift should be around 23%. We observe, however, values for the

drift around 40% for time scales around 3 minutes (Fig. **V-7**). For these time scales, some particles diffusing backwards should be observed. An effect comes into play here to prevent backwards diffusion of the particles.

This effect is the hydrodynamic interactions between particles. Just after switching off the AC field, the particles are still gathered in this banana shape structure shown in Figure **V-6**. They first diffuse faster to the right (to the forwards well) than backwards, because the distances are different. Once there, they prevent the other particles to diffuse backwards. This steric repulsion explains why we almost never observe any particle diffusing to the backwards well. This pump, by suppressing the backwards drift, is more efficient than the thermal ratchet in Chapter IV.

This poses the question of the value of the drift at saturation (long off times): It should not be 1/2 because the diffusion is now two-dimensional as opposed to the one-dimensional diffusion of Chapter IV. It should be closer to 1/4 (because of the four principal directions to diffuse). From fitting equation (Vi) to the experimental points, and allowing the multiplicative factor in front of the exponential to be a free parameter, the saturation value is obtained to 0.56, surprisingly close to (1/2). The hydrodynamic interactions between particles described above seem to be strong enough to enhance the drift by almost a factor of two. Note that similar measurements (Rousselet 1994) of the drift in the case where the particles were trapped at the tips (see Figure **V -5**) indicated a saturation value close to 0.9!

B 4 Particle separation

One could use this device for particle separation. Particles of different diameters will have different diffusion coefficients, and the characteristic time scale for the drift will be different. Figure **V - 8** shows a suspension of silica spheres of two different diameters (1.5 and 2.5 microns) diffusing freely when the AC field is switched off.

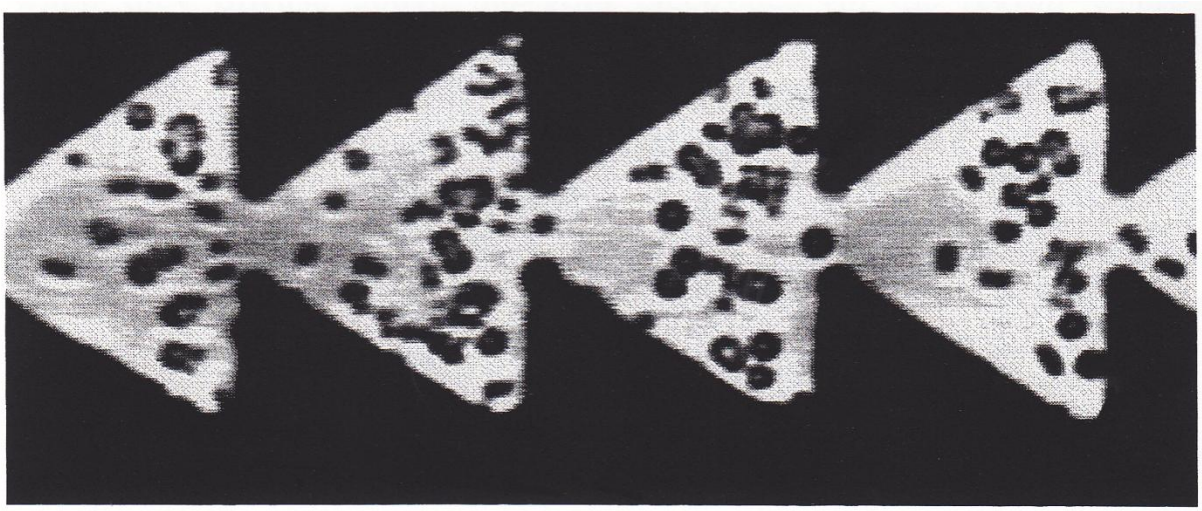

Figure **V -8**: The freely diffusing 1.5 and 2.5 microns diameter silica particles (the potential is switched off). Full horizontal scale=70 microns. The black triangles represent the gold electrodes. Particles induced motion is from left to right.

Figure **V-9** shows the drift as a function of the off time τ_{off} for the two kinds of particles. The solid lines are fit of equation (V1) to the experimental points. They yield two characteristic times, of order 130 seconds and 380 seconds. Note that particle separation is maximum for times around 100 seconds, where the drift of 1.5 microns diameter particles is already significant (around 10%), but where the drift of 2.5 microns diameter particles is one order of magnitude smaller (around 1%).

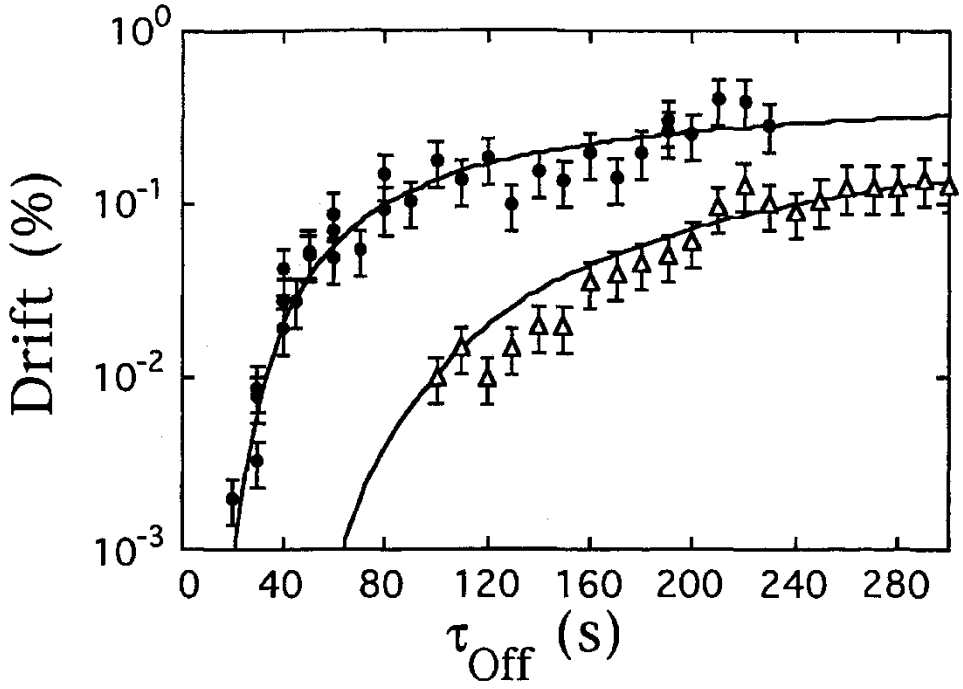

Figure **V-9**: the drift as a function of the off time in seconds for silica particles of diameter 1.5 microns (black dots) and 2.5 microns (triangles). The solid lines are fits of equation (Vi) to the experimental points.

Note that the ratio of the two characteristic times (130 s and 380 s) is around 3, whereas the ratio of the particle diameters is only 1.7. This indicates a non trivial scaling between the two curves: the diffusion length $\lambda_f = \sqrt{2D\tau_f}$ is different for the two particles (λ_f is around 5 microns for the small spheres and around 6.7 microns for the large ones). It means that the potential profile is also function of the particle diameter (Rousselet 1994).

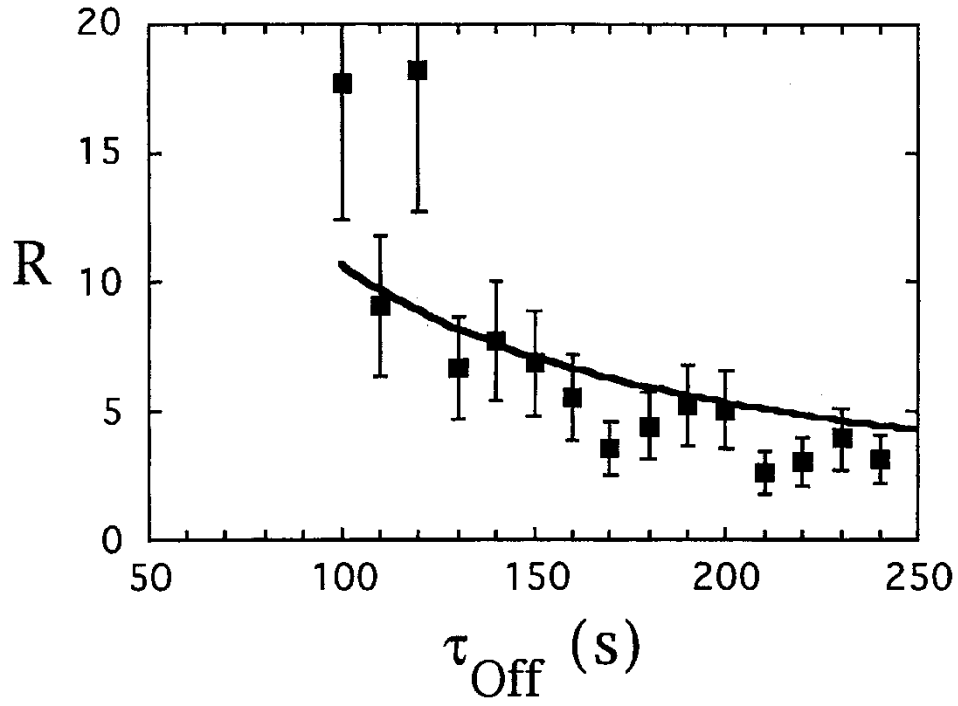

Figure **V - 10**: The ratio of the drifts of two different diameter particles (1.5 µm and 2.5 µm), as a function of the off time τ_{off}.

The ratio R of the two drifts is plotted in Figure **V -10** as a function of the off time τ_{off}. Particle separation is maximum for time scales around 100 seconds. From a Taylor expansion of equations (IV2a) and (IV2b) as a function of the small parameter τ_{off}^{-1}, one gets that the ratio of the two drifts decreases slowly back to zero as a power law of exponent -1 as the off time goes to infinity. This is the solid line in Figure **V-10**. It is not fitted to the experimental points.

In conclusion, we built with lithography techniques a dielectrophoretic pump on the principles of the thermal ratchet described in Chapter IV. The advantage of lithography above optical tweezing is the simplicity of the experimental setup: one need only connect a function generator to the electrodes to observe an induced drift of Brownian particles. Hydrodynamic interactions between particles are shown to enhance the efficiency of' this pump. The measured drifts are surprisingly well approximated by the simple equation (V1) derived in Chapter IV in the one dimensional case. Particle separation using this technique is possible. A complete understanding of the role of hydrodynamic interactions, as well as of the dependence of the potential profile upon the particle diameter, is still lacking.

More generally, spatial separation of Brownian particles using the thermal fluctuations is possible. This segregation does not violate any, deep thermodynamics principles: the system is periodically forced at a given off time τ_{off}. This external forcing extracts out components of the particle spatial fluctuations in resonance with the two different diffusive length scales λ_f and λ_b. This induces a net drift. Because the Brownian trajectories are different for particles of different sizes, the value of the drift will also be different, allowing separation according to the size.

Summary and Conclusion

This thesis has focused on the interplay between dynamics (trajectories) and thermodynamics (drift and diffusion current, probability density) of Brownian motion. In chapter II and III, as well as in Appendix C, we showed that relevant informations about potential and hydrodynamic interactions can be extracted from the intrinsically noisy trajectories of a Brownian particle. In chapter IV and V, we showed how these trajectories can be affected by modulating in time and space a localized trapping potential. In particular, a net drift of Brownian particles is induced from the time modulation of a periodic asymmetric potential, along the lines of a thermal ratchet.

Potential interactions are shown in Chapter II to be fairly easy to include in the theory of Brownian motion. In the case of an isothermal fluid, the equilibrium probability density is always the Boltzmann distribution. In appendix C, direct observation of the depletion forces exerted by a sea of 35 nm diameter spheres on a 1 micron diameter particle near a wall is reported. A statistical analysis of the local variance along the trajectories yields a measurement of the mean escape time from the entropic trap.

Taking into account hydrodynamic interactions is more subtle. Depending on the physical system, three choices for Fick's law are possible. These choices are formally analogous to the three conventions (including Ito and Stratonovitch) one has to choose when writing a Langevin-type equation for the particle's position. The two issues are however shown in Appendix B to be two distinct and separate problems.

In Chapter III, real time processing of the trajectories of micron sized spheres between two plates is reported. The horizontal diffusion coefficient is measured from averaging the square of the particle displacement over many trajectories. These measurements deviate from the Stokes-Einstein law, derived in

Chapter I in the case of a free particle. This is due to the hydrodynamic interactions between the particle and the bottom plate of the cell. These deviations (as much as 1/3) are shown to be function of a single dimensionless position parameter. Comparisons with theoretical estimates confirm that Fick's law in the case of an isothermal fluid with a spatially varying viscosity is still written:

$$\vec{J}_d = -D(\vec{x})\vec{\nabla}P(\vec{x},t)$$

In Chapter IV, the technique of optical tweezer is used to create a localized trap that we move in space and modulate in time. Three regimes of particle motion are observed as a function of the trap velocity. At low velocities, the particle follows deterministically the trap. At intermediate velocities (between 20 µm/s and 1000 µm/s for a 1.5 microns diameter sphere in water), the trapping force is not strong enough to hold the particle in the trap. This one escapes, but is, however, slightly displaced. The mean particle displacement scales with the inverse square of the trap velocity. At high velocity, thermal fluctuations dominate and no net particle displacement is observed. The diffusion of the particle is, however, confined to the one dimensional pattern laid out by the motion of the trap. This opens the possibility to study the statistics of Brownian particles in confined geometry.

We thus built an optical "thermal ratchet": by modulating the beam intensity, we create along a circle a periodic asymmetric potential. By switching on and off this spatial modulation, we induce a net drift of Brownian particles. This effect surprised us at first: because the potential is periodic, the net force on the particles is zero. The value of the drift shows a resonance as a function of the off time. Particle separation using this device is however unpractical: one can trap only one particle at a time, and the maximum value of the drift probability is only 15%.

This problem is overcome in Chapter V, where we built a thermal ratchet by depositing gold electrodes on a glass plate. Here, the potential is created by applying an AC electric field (100 kHz) between the two electrodes. One can trap more than one particle at a time. As a result, hydrodynamic interactions between particles are shown to enhance by a factor two the efficiency of such a device. Their precise role, as well as the dependence of the potential profile upon the particle diameter, need to be further quantified. In any case, by periodically switching on and off a spatially periodic asymmetric potential, one induces a spatial segregation of Brownian particles according to their sizes. This surprising effect shows that the thermal fluctuations can be harnessed into producing a net motion.

This thesis was motivated, in addition to the author's obvious fascination for random walks, by a rather simple observation: on the macroscopic scale where we live, forces, and especially the connection between the forces and the resulting trajectories, are well defined. However, as one goes down to the micron scale, where thermal noise dominates most of the behavior, things are not so clear: Hydrodynamic interactions can induce particles drift but cannot be casted into a usual force. We saw indeed that their effects on the Brownian trajectories was quite subtle. The localized optical trap that we move in space and time (Chapter IV) is useful in understanding at a deeper level the connection between the force and the trajectories. Here, by increasing the trap velocity, one goes continuously from the classical deterministic regime to the freely diffusive one. In between, the forcing weakens with the trap velocity as a power law predicted by a simple stochastic model. It would be nice to beyond this scaling argument, both experimentally and theoretically, so as to extend our grasp into this region where what we think is noise can induce motion (as in a thermal ratchet), and where forces stop being relevant. Colloidal suspensions seem to offer in that regards the ideal playground to address such questions.